

Review

# Physical Properties of the NbC Carbide

Marcio Gustavo Di Vernieri Cuppari <sup>\*,†</sup> and Sydney Ferreira Santos <sup>†</sup>

Universidade Federal do ABC, Av. dos Estados, 5001, Santo André, SP 09210-580, Brazil;  
sydney.ferreira@ufabc.edu.br

\* Correspondence: marcio.vernieri@ufabc.edu.br; Tel.: +55-11-4996-0146

† These authors contributed equally to this work.

Academic Editor: Jordi Sort Viñas

Received: 10 June 2016 ; Accepted: 27 September 2016; Published: 21 October 2016

**Abstract:** Transition metal carbides are interesting materials with a singular combination of properties, such as high melting points, high hardness, good transport properties and relatively low costs, which makes them excellent candidates for several technological applications. The possible applications of NbC carbide remained unexplored as it was in the past expensive and available in limited volumes. In order to guide investigations of the applicability of NbC, a deeper understanding of the physical properties of this carbide is fundamental. In this review paper, key physical properties of NbC are compiled with emphasis on its chemical bonding, a careful description of the C-Nb phase diagram, the phases formed and the crystal structures. Thermal properties are discussed and correlated with the intrinsic and extrinsic features of NbC. Finally, elastic properties are discussed.

**Keywords:** niobium carbide; chemical bonding; crystal structures; elastic properties; thermal properties

## 1. Introduction

Transition metal carbides are metallic compounds with a very unique combination of physical properties: high melting point, high hardness and high thermal and electrical conductivities. These properties make them suitable candidates for applications like cutting and grinding tools, hard electrical contacts, cylinder linings and diffusion-resistant thin-film coatings of microcircuit devices [1]. This combination of physical properties indicates a complex chemical bonding between the metallic element and carbon, and yet, the crystalline structure of the carbides is simple, typically of the NaCl type or hexagonal, as is observed for the carbides of the early transition metals Groups 4 (Ti, Zr, Hf) and 5 (V, Nb, Ta) [2,3].

Metal carbides have been extensively studied since the early 1960s, and the main characteristics of these materials can now be explained in view of their crystal structures and chemical bonding, although there are some phenomena relating to these carbides that are not fully understood until today. Transition metal carbides, such as TiC and WC, have remarkable technological relevance and are largely used in industry. Unlike other transition metal carbides, the technological use of NbC has been neglected over time, although this compound influences the microstructural evolution during the processing and final properties of steels and cast irons.

For instance, Llanos et al. [4] reported strain-induced NbC precipitation that resulted in softening retardation during the thermomechanical processing of a high-Mn twinning-induced plasticity (TWIP) steel microalloyed with Nb processed at 1000 °C. Similar results were reported by Li et al. [5] studying another Nb-microalloyed TWIP steel after a sequence of heat treatments and cold rolling steps. For hypereutectic high chromium cast irons, Zhi et al. [6] reported that the addition of Nb led to the formation of NbC carbide during the solidification, reducing the carbon content in the liquid, which in turn resulted in carbide refinement and changes in the morphology of the  $M_7C_3$  primary carbide, which became more isotropic. Despite the emphasized importance of NbC in ferrous alloys, only

recently, the use of pristine NbC or NbC-rich materials has gained attention. Woydt et al. [7] ascribed this late interest in NbC applications to its poor sinterability, which can be overcome by modern sintering techniques, such as spark-plasma sintering (SPS), hot pressing, etc. [7,8]. These authors successfully sintered binderless NbC and Co bonded NbC (8% volume of Co) by hot pressing and spark-plasma sintering, respectively, and performed mechanical characterization, microstructural analyses and wear tests in different experimental conditions observing that both pristine NbC and bonded NbC-8% Co presented high wear resistance, which allow them to compete with several typical hard metals and ceramics.

Another potential application for NbC-based materials is electrical contact coatings [9]. Typically, electrical contacts are coated with a noble metal with very low electrical resistance, but with high costs and poor wear resistance. NbC is electrically conductive and in combination with its wear resistance is potentially suited for electrical contacts, which normally suffer fretting wear.

Nanocomposites of nanocrystalline (nc) metal carbides (nc-TiC, nc-ZrC), dispersed in an amorphous matrix (amorphous carbon or amorphous SiC) are under investigation, but a better performance was reported (lower resistivity) of NbC<sub>x</sub>/amorphous carbon nanocomposite films when compared to similar nanocomposite films. Cu/Nb composites are also under investigation, especially using non-conventional processing techniques (severe plastic deformation) and the design of microstructures (nanocomposites, functional graded composites, etc.) [10,11].

More recently, transition metal carbides started to be considered as candidates for electrochemical energy storage and conversion applications due to their electrochemical activities in several reactions of interest associated with their insignificant costs, when compared to Pt and Pt alloy nanoparticles widely used for these kinds of applications. These carbides, including NbC and NbC-based materials, have been tested as electrode materials in Li-ion and Na-ion rechargeable batteries, electrochemical supercapacitors and electrochemical reactions as hydrogen evolution reaction (HER), oxygen reduction reaction (ORR) and oxygen evolution reaction (OER). These electrochemical reactions are important for fuel cells and electrolyzers [12]. In these applications, a wide range of different nanostructures are under investigation, like hollow nanofibers, nanorods, nanopillars, nanotubes, hierarchical nanostructures, nano-clothes, MXenes(2D nanostructures obtained by etching MAXphases), among many others [12–14].

The practical application of NbC in all areas mentioned above requires a strong background on its fundamental properties, which motivated us to prepare this manuscript to present a critical review of the physical properties of the NbC published in the literature. First, a short overview of the C-Nb phase diagram will be given in order to present the main phases of this system and their crystal structures. Then, an overview of the main features of the chemical bonding of these compounds will be given. Next the physical properties will be discussed beginning with the study on how the lattice parameter of the NbC varies with vacancy concentration followed by its thermal properties. Finally, the elastic properties will be discussed.

## 2. The C-Nb Phase Diagram

There are several versions of the C-Nb phase diagram published in the literature, both from experimental information [15–18], as well as from thermodynamic assessments using the CALPHAD (Computer Coupling of Phase Diagrams and Thermochemistry) protocol [19–25]. Some features of the C-Nb system are not completely understood, especially the order-disorder transformations present in this system. Smith et al. [17] critically reviewed the experimental information available on the C-Nb system and proposed the phase diagram shown in Figure 1.

This diagram shows four different carbides: the  $\gamma$ -Nb<sub>2</sub>C with the hexagonal structure, which transforms to an ordered hexagonal phase,  $\beta$ -Nb<sub>2</sub>C, at lower temperatures, the NbC<sub>1-x</sub> with a NaCl-type structure, which transforms to an ordered carbide Nb<sub>6</sub>C<sub>5</sub> at approximately 1050 °C and the Nb<sub>4</sub>C<sub>3-x</sub> carbide, which is very similar to the ordered phase of the C-V system, V<sub>6</sub>C<sub>5</sub>.

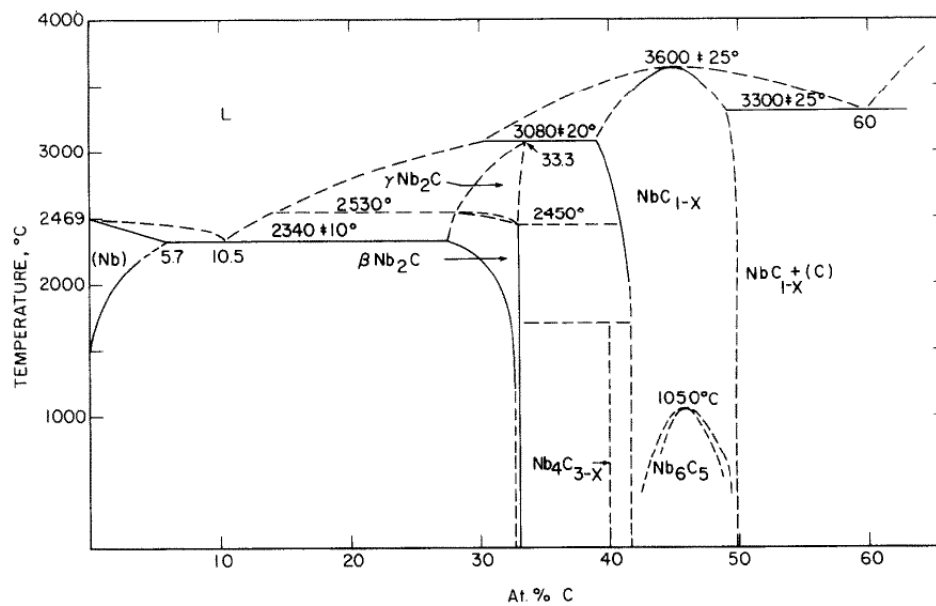


**Figure 1.** Phase diagram of the C-Nb system [17]. Adapted from Smith et al. *J. Nucl. Mater.* **1987**, *148*, 1–16. Copyright © 1987 with permission from Elsevier.

The phase diagram presented in Figure 1 indicates that the  $\gamma\text{-Nb}_2\text{C}$  carbide is formed through a peritectic reaction occurring at 3080 °C. With decreasing temperature, the (Nb) +  $\beta\text{-Nb}_2\text{C}$  boundary changes its curvature rapidly narrowing the homogeneity range of the  $\beta\text{-Nb}_2\text{C}$ , and this phase can be considered a stoichiometric phase at temperatures below 1500 °C. The crystalline structure of the  $\gamma\text{-Nb}_2\text{C}$  belongs to the  $P6_3/mmc$  space group (space group number 194) with the prototype structure of the  $W_2\text{C}$  phase [17]. Its stacking sequence can be described as AbAb where A refers to the metallic atoms and b refers to the carbon atoms [2,26]. The ordered  $\beta\text{-Nb}_2\text{C}$  belongs to the  $P\bar{3}1m$  space group (space group Number 162).

The  $\text{NbC}_{1-x}$  carbide is formed by congruent melting at 3600 °C, as shown in Figure 1, and it has a wider homogeneity range when compared to the  $\text{Nb}_2\text{C}$ . The NbC crystal structure is isomorphic to the NaCl (space group  $Fm\bar{3}m$ ; Number 225) which can be viewed as two interpenetrating fcc lattices (see Figure 2). In one of these sub-lattices, the positions are occupied by metallic atoms and in the other by carbon atoms. The stacking sequence of this phase can be described as AbCaBc, where A, B or C refer to the metallic atoms and a, b or c to the carbon atoms [26]. The atoms in this structure have octahedral coordination, and the carbon atoms occupy half of the octahedral interstices of the metallic sub-lattice [3]. At temperatures around 1050 °C, there is a order-disorder reaction resulting in a carbide with stoichiometry  $\text{Nb}_6\text{C}_5$  and trigonal structure (space group  $P3_1$ ) [3,17,27–36]. In this carbide, atomic planes with and without defects are stacked alternately [3]. The studies about the order-disorder reaction of the  $\text{Nb}_2\text{C}$  carbides are incomplete [37] compared to the work done on the  $\text{Nb}_6\text{C}_5$  phase.

The presence of the  $\text{Nb}_4\text{C}_{3-x}$  as the stable phase of the C-Nb system is a controversial issue. Smith et al. [17] in their review present experimental results where this phase appears to be a stable one. However, various other researches cited in the same paper were not able to verify the existence of this phase. It seems that this phase is formed through a peritectoid reaction between the NbC and  $\text{Nb}_2\text{C}$  phases, as shown in Figure 1. More recently, Wisenberger et al. [18] studied the V-C, Nb-C, Ta-C and the Ta-N binary systems using the diffusion couple technique, and their results show that the formation of this phase is very slow and is influenced by the crystallographic orientation of the  $\text{Nb}_2\text{C}$ . In order to avoid some of these limitations, the authors decided to study the decomposition temperature with hot-pressed specimens with compositions in the range of 36.0–39.0 at. % C annealed at different temperatures up to 1650 °C for 40 h. By using this method, the presence of the  $\text{Nb}_4\text{C}_{3-x}$

phase was observed in samples annealed at 1547 °C and was absent in samples annealed at 1602 °C. The authors then suggested a peritectoid decomposition temperature of 1575 °C and composition range between 40.1 and 40.7 at. % C.

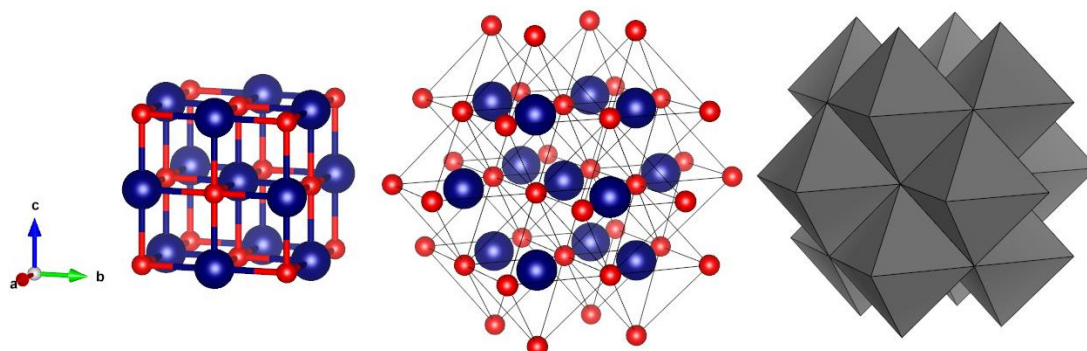


**Figure 2.** Schematic representation of the B1 structure of the NbC carbide (left) and coordination octahedra. Figure prepared with VESTA [43].

### 3. Chemical Bonding

The chemical bonding in transition metal carbides is of a complex nature with a covalent, metallic and ionic character. This fact explains the observed physical properties: high hardness and high melting points are properties typical of solids with ionic or covalent bonding, while thermal and electrical conductivity are characteristics of metallic bonding. The electronic structure of the transition metal carbides was extensively studied in [38] and in several other papers [39–42]. It is firmly established in the literature that the main characteristic of the chemical bonding in transition metal carbides is a covalent bonding with hybridization of the  $2p$  orbitals of the carbon atoms and  $d$  orbitals of the metallic atom [38].

As already pointed out in the preceding section, in the NbC carbide, the metallic and non-metallic atoms have an octahedral coordination. For this reason, we can think of this octahedron as a construction unit of the B1 structure with a formula  $MX_6$  (or equivalently,  $M_6X$ ), where  $M$  represents the metallic atoms and  $X$  the carbon atom. In the NbC carbide, these octahedra are connected through their edges, as shown in Figure 2.

The valence shell of the Nb atom has partially occupied  $d$  orbitals (electronic configuration  $[Kr]4d^45s^1$ ), and those orbitals are the ones that participate in the chemical bonding with the carbon  $p$  orbitals. The isolated Nb atom has degenerated  $d$  orbitals with the same energy. The bond formation between Nb and C can be pictured if we imagine that the metallic atom occupies the central position in the interior of the octahedron and the six carbon atoms approach the Nb in three mutually perpendicular directions. Given the symmetry of the  $d$  orbitals and considering the carbon atoms as negative point charges, some of the  $d$  orbitals interact more strongly with the carbon orbitals than the ones less favorably oriented. The orbitals  $d_{z^2}$  and  $d_{x^2-y^2}$  are oriented according to the  $x$ ,  $y$  and  $z$  axis where the carbon atoms are located, and the electrons in these orbitals are subjected to a greater repulsion caused by the carbon atoms [44]. This lifts the degeneracy of the  $d$  orbitals, and they separate into two energy levels: the orbital with higher energy are called  $e_g$  orbitals and correspond to the  $d_{z^2}$  and  $d_{x^2-y^2}$  orbitals, and the low energy orbitals are called  $t_{2g}$  and correspond to the  $d_{xy}$ ,  $d_{yz}$  and  $d_{xz}$  orbitals. The orbitals with  $e_g$  symmetry of the Nb atom and some of the carbon  $p$  orbitals participate more actively in the chemical bonding, forming a hybridized  $pd_\sigma$  bonding. The remaining Nb  $d$  orbitals form another kind of bonding,  $dd_\pi$ . Therefore, it is possible to explain the physical properties of the transition metal carbides through an analysis of their chemical bonding. The  $pd_\sigma$  bonds are very strong and highly directional and are responsible for the high hardness and high melting points. On the other hand, the  $dd_\pi$  bonds, although with little contribution to the cohesion [38], are responsible for the observed transport properties (electric and thermal conductivity). It should be

noted that there is also some charge transfer of the metallic electrons to the carbon atom, which gives an ionic characteristic to the bonding. In the Nb<sub>2</sub>C carbide, the metallic bonding is more important and contribute more to the solid cohesion [38].

Most of the studies on the electronic structure of the transition metal carbides are conducted with stoichiometric composition and do not consider the effects of vacancies. Experiments or theoretical studies concerning the effects of the vacancies on the electronic structure and bonding of the transition metal carbides are more scarce. It is known that the vacancies can distort the crystal structure and change the chemical bonding in the vicinity of these defects. Generally speaking, a higher vacancy concentration (or a lower carbon content) increases the number of the M–M bonds and diminishes the covalent character of the bonding [45–48]. However, there are some results published in the literature that contradict this statement [49,50].

## 4. Physical Properties

### 4.1. Lattice Parameter

Experimental results [3,29,51–57] presented in Figure 3 indicate that the lattice parameter increases with the carbon content in a nonlinear manner.

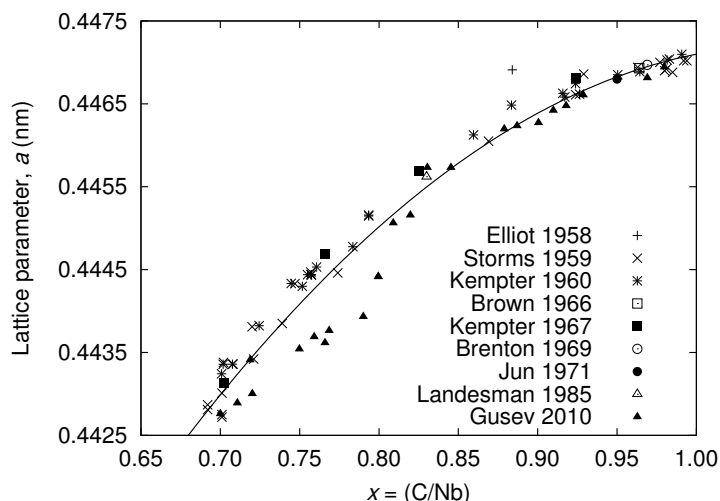


**Figure 3.** Variation of the NbC lattice parameter with carbon content. Experimental data taken from [29,51–57].

Gusev [3] discusses the results shown in Figure 3 considering the presence of vacancies in the carbon sub-lattice. He argues that vacancies present in the structure of the transition metal carbides break the translational symmetry of the lattice and induce a displacement of the atoms in relation to their positions in a perfect lattice. These displacements are not due to thermal vibrations and occur because of an asymmetric distribution of the chemical bonding in those regions and different bond energies [3]. The size of the octahedral interstice is smaller than necessary to accommodate the carbon atom without straining the structure and displacing the metallic atoms outwards. Once the vacancy is created, the Nb atoms would be displaced towards the interstice, causing the lattice parameter contraction with higher vacancy concentration (lower carbon content). However, experimental studies [28,32,58,59] show that the Nb atoms are displaced away from the vacancy, and if this were the only effect of the vacancy on the structure, the lattice parameter should increase for higher vacancy concentrations. Since this conclusion contradicts directly the results shown in Figure 3, the displacement of metallic and nonmetallic atoms beyond the first coordination shell of the vacancies has to be taken into account. The carbon atoms have octahedral coordination; the presence of a carbon vacancy in the structure creates a geometric condition for the metallic atom to

be displaced towards the interstice. However, this movement is restricted because of the C-Nb bond in the adjacent octahedron, and this bond is responsible for the observed displacement of the Nb atom, expanding the central interstice. In order to reconcile this observation with the fact that the lattice parameter decreases for lower vacancy concentrations, the atoms beyond the first coordination shell of the vacancy must be displaced towards the interstice, decreasing the lattice parameter as shown in Figure 3. The displacement caused by the vacancies must extend through distances greater than the lattice parameter, and it is reasonable to assume that this perturbation decreases with distance. For a lower vacancy concentration, these displacement fields do not overlap, and the lattice parameter increases. For a higher vacancy concentration, the displacement fields start to interact, canceling each other, causing an expansion of the lattice parameter. As a result, a relationship between vacancy concentration and the lattice parameter would show a maximum, which is not evident in Figure 3. This could mean that the attenuation of the displacement field extends through distances that allow them to be overlapped between them. The same behavior shown in Figure 3 was obtained by DFT calculations made by Zaoui et al. [60] when vacancies were explicitly taken into account.

The explanation above is a qualitative analysis of the experimental results. One also has to consider that the specimens always show some degree of inhomogeneity and might be composed of a mixture of different carbides leading to non-stoichiometry. If the specimen is composed of a mixture of different phases, the lattice parameter can be calculated as a weighted average of the lattice parameters of the different carbides present in the specimen.

#### 4.2. Density

There is no systematic study concerning the density of the NbC carbide with chemical composition or temperature. The published data are calculated from measurements of the lattice parameter used to compare the density of sintered specimens with the theoretical value. Fortunately, there is a wealth of data published in the literature that allow some considerations about the NbC density to be made. The density of the stoichiometric NbC can be calculated from the following equation:

$$\rho = \frac{m}{V_c} \quad (1)$$

The atomic mass is given by:

$$m = \frac{N_C M_C + N_{Nb} M_{Nb}}{N_0} \quad (2)$$

For a stoichiometric composition, we have  $N_C = N_{Nb} = 4$ . Since there are no vacancies in the metallic sub-lattice and knowing the C/M ratio of the carbon and metal atoms, we can write:

$$m = \frac{4(xM_C + M_{Nb})}{N_0} \quad (3)$$

The unity cell volume can be calculated from the data presented in Figure 3. Using the least square method, an equation relating the lattice parameter with carbon content can be obtained:

$$a = 0.410392 + 0.0695707x - 0.0328634x^2 \quad (4)$$

where  $a$  is given in nanometers (nm). Empirical relations similar to Equation (4) can be found in the literature [17,52,53]. Finally, the NbC density can be calculated from Equations (3) and (4). Figure 4 shows how the NbC density,  $\rho$ , varies with the C/Nb ratio in comparison with the results of [61].

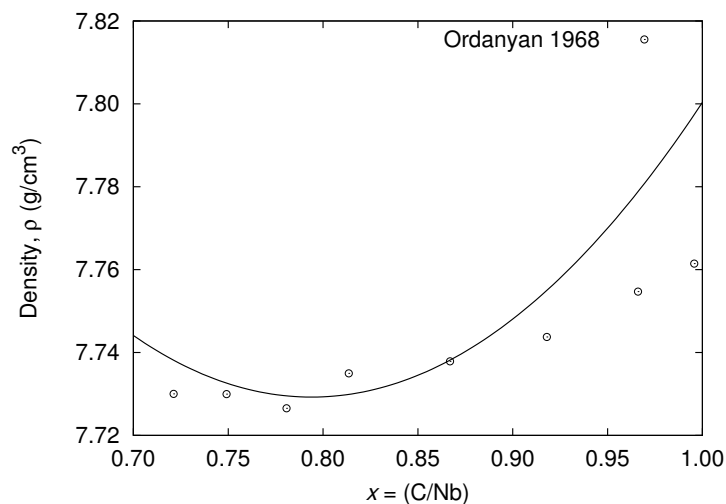


**Figure 4.** NbC density variation with stoichiometry.

The results presented in Figure 4 show that the NbC density diminishes at first and then increases with the carbon content, passing through a minimum when  $x$  reaches approximately 0.78. The density range is relatively narrow, from 7.73–7.80 g/cm<sup>3</sup> approximately. For lower carbon concentrations, the influence of the lattice parameter on the density is more pronounced than of the mass of the carbide. It is interesting to note that the plot presented in Figure 4 shows a well-defined minimum, while the data shown in Figure 3 do not. Figure 4 also compares the calculated density with the experimental results (calculated using the lattice parameter measured from X-ray diffraction) published in [61]. The agreement between calculated and experimental values is acceptable considering the large errors associated with density measurements.

#### 4.3. Thermal Properties

Figure 5 shows how the NbC lattice parameter varies with the temperature using specimens with different chemical compositions as measured by X-ray diffraction. These results indicate that the lattice parameter increases linearly with temperature, and the chemical composition has little influence on this parameter, since all curves shown in Figure 5 have almost the same rate of increase in  $a$  with temperature. The most striking difference between the data shown in this figure concerns the results for the NbC<sub>0.884</sub> obtained by Elliot [51] and of the NbC<sub>0.924</sub> measured by Kempter [55], which indicate the same lattice parameter at room temperature for these two compositions. The relative expansion of the lattice parameter with temperature, obtained by means of dilatometric measurements,  $\Delta a/a$ , is shown in Figure 6 and confirms that the chemical composition has no influence on the lattice parameter variation with temperature.

Although the different measurements for the lattice parameter variation with temperature for the NbC carbide found in the literature are in good agreement, the published values for the volumetric thermal expansion coefficient measured by different authors are in poor agreement. The volumetric thermal expansion coefficient is defined as:

$$\alpha_V = \frac{1}{V} \frac{dV}{dT} \quad (5)$$

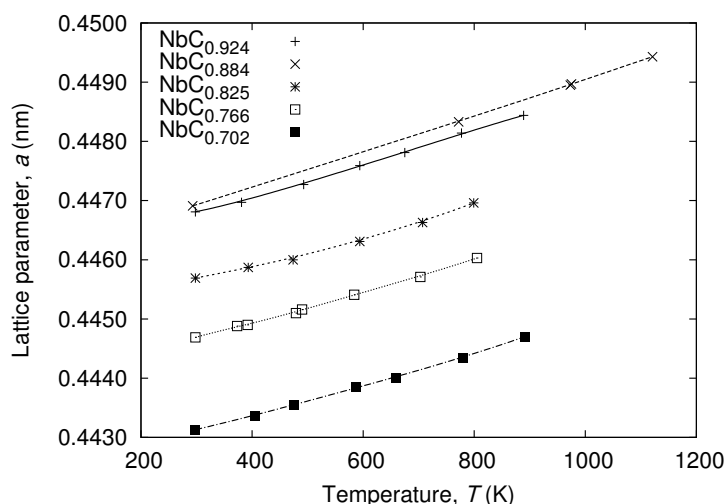


**Figure 5.** Lattice parameter of the NbC carbide as a function of temperature for different stoichiometries [51,55].

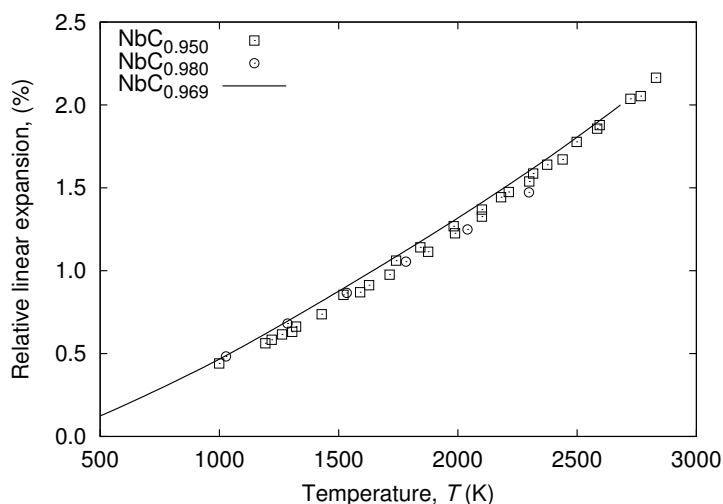


**Figure 6.** Relative linear expansion of the NbC carbide lattice parameter as a function of the temperature for different stoichiometries [56,57].

The procedure employed to obtain  $\alpha_V$  involves the calculation of a derivative, which can amplify experimental errors. The most common error sources in these measurements are those related to the production of specimens with heterogeneous chemical composition and chemical composition changes during the tests (oxidation) [62]. Another source of error is the sintering of the specimens during the test when dilatometric methods are used to measure the thermal expansion. Figure 7 [62] shows that the volumetric thermal expansion coefficient of the NbC carbide varies in a nonlinear manner with the temperature and has an inflexion point at approximately 1000 K. The author did not mention the chemical composition of the carbide used for this measurement. The same work [62] presents some data concerning the variation of  $\alpha_V$  with changes in chemical compositions at 800 K (Figure 8), and this result indicates that the thermal expansion of the NbC carbide increases with the carbon content. A completely different result is presented by Samsonov [63] (Figure 9), which indicates that the linear thermal expansion coefficient of the NbC carbide has a parabolic variation with composition. The author did not indicate the temperature at which those measurements were performed. It is clear from these comments that a systematic investigation of the thermal expansion of the NbC carbide is lacking in the literature.

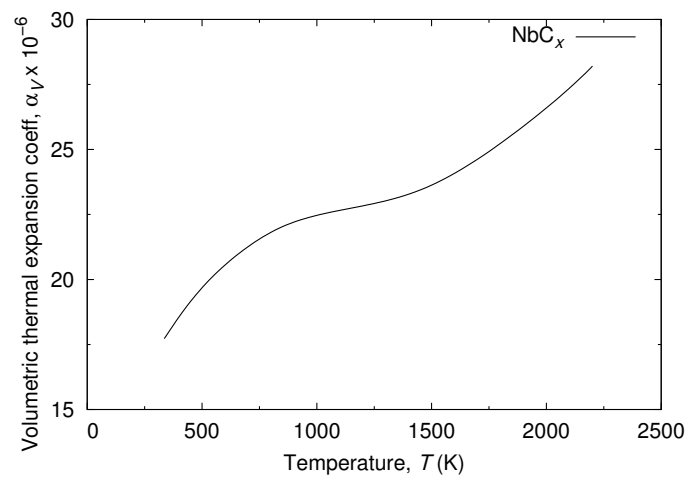


**Figure 7.** Volumetric thermal expansion coefficient of the NbC carbide as a function of the temperature [62].

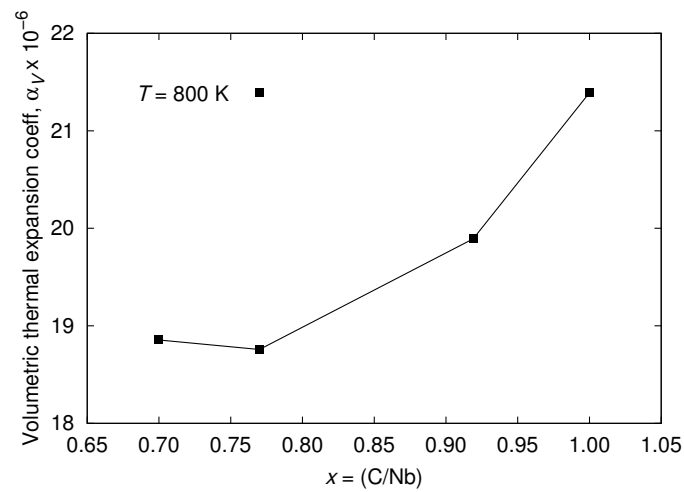


**Figure 8.** Volumetric thermal expansion coefficient of the NbC carbide for different chemical compositions [62].

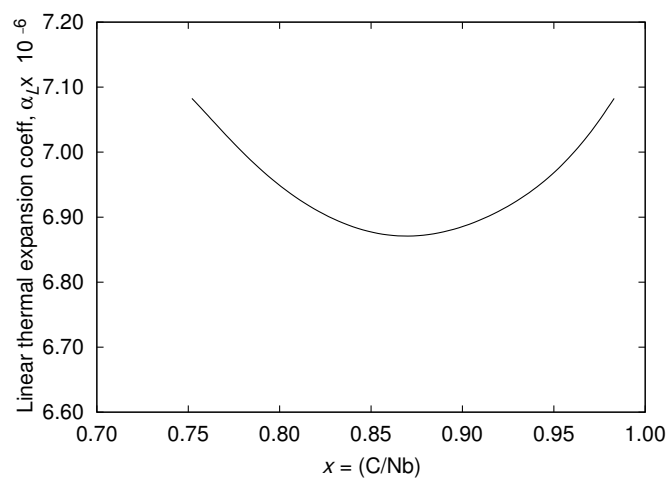


**Figure 9.** Thermal expansion coefficient of the NbC carbide for different chemical compositions [63].

Since the most reliable information available about the thermal expansion of the NbC carbide is the measurements of the lattice parameter presented in [51,55–57], these data were used to calculate an average linear expansion coefficient,  $\bar{\alpha}_L$ , defined as:

$$\bar{\alpha}_L = \frac{1}{\Delta T} \frac{\Delta L}{L} = \frac{1}{\Delta T} \frac{\Delta a}{a} \quad (6)$$

and the results are shown in Table 1. The average thermal expansion coefficient of the NbC carbide is not independent of the chemical composition, although it is difficult to establish an exact relationship between them. Kempter and Storms [55] restricted the analysis of their results to temperatures up to 600 °C and claimed that the thermal expansion coefficient increases with the carbon content. However, this relationship could not be verified for higher temperatures.

**Table 1.** Average thermal expansion coefficient.

C/Nb Ratio	$\bar{\alpha}_L$	Reference
0.980	7.81	[64]
0.969	8.53	[56]
0.924	6.17	[55]
0.884	6.81	[51]
0.825	5.69	[55]
0.766	5.94	[55]
0.702	5.97	[55]

Figure 10 shows the variation of the molar heat capacity with the temperature at constant pressure of the NbC<sub>0.970</sub> carbide. For high temperatures, above approximately 1200 K, the molar heat capacity varies almost linearly with temperature. For lower temperatures, it decreases rapidly. The chemical composition has little effect on this property. For different compositions and for temperatures up to 300 K, the molar heat capacity of the carbide appears to increase for larger carbon content, as shown in Figure 11.

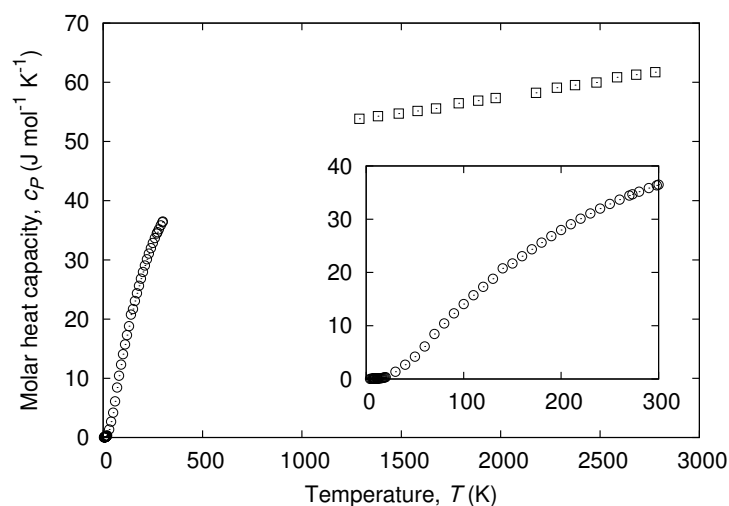


**Figure 10.** Specific heat of the NbC<sub>0.970</sub> carbide as a function of the temperature. The data for high and low temperatures are given in [3,65], respectively.

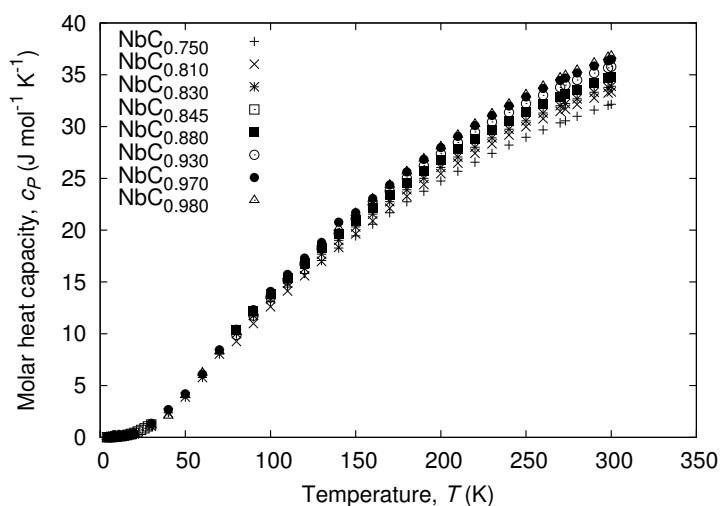


**Figure 11.** Specific heat of the NbC carbide with temperature for different carbon contents [3].

#### 4.4. Elastic Properties

Transition metal carbides are materials with high hardness and are extremely brittle, which makes the production of specimens with a complex geometry, such as the ones required for the mechanical tests, very difficult. For this reason, the mechanical properties of these materials are usually measured by ultrasonic methods with sintered or isostatically-pressed specimens [66]. In these tests, the Young modulus,  $E$ , and shear modulus,  $G$ , are calculated from measured longitudinal and transversal sound speeds in the materials, and other properties, like Poisson coefficient,  $\nu$ , and bulk modulus,  $B$ , are calculated from these. The advantage of this combination of fabrication route and ultrasonic testing is that these tests require specimens with a simple geometry that can be easily obtained by sintering. However, the results will depend strongly on the porosity level attained, and reliable results require test specimens with porosity levels below 5% or 6% [66]. There is also the possibility of using monocrystals for these measurements [67], but this is not a very common method given the difficulties in producing crystals of materials with high melting points from the liquid state. Either way, there are numerous results of mechanical properties of the transition metal carbides published in the literature, and Table 2 shows typical values for some of the elastic properties of the NbC carbide with different chemical compositions at room temperature.

**Table 2.** Elastic properties of the NbC carbide at room temperature.

C/Nb Ratio	Young Modulus $E$ (GPa)	Shear Modulus $G$ (GPa)	Bulk Modulus $B$ (GPa)	Poisson Ratio $\nu$	Reference
0.865	438	178	267	0.23	[67]
0.964	488	198	300	0.22	[54]
0.969	492	202	291	0.22	[56]

It should be noted that the some of the mechanical properties presented in this section were taken from results published in the 1960s and 1970s. At that time, modern sintering techniques were not available, and specimens from these studies sometimes presented porosity levels around 5%. Nowadays, the use of sintering techniques like spark plasma sintering provides accelerated densification compared to regular sintering [68], which makes the porosity a lesser problem. For instance, [69] indicates a porosity level of approximately 2%, even for binderless NbC. Therefore, the data below include the porosity level of the specimens to facilitate the comparison of the results obtained by different researchers.

Speck [66], Brenton [56] and Jun [70] studied the variation of the Young modulus with temperature, and their results are shown in Figure 12. The increase in temperature causes a decrease in the Young modulus for all chemical compositions. The results obtained by Brenton [56] and Jun [70] are very similar despite the difference in the chemical composition, which seems to confirm the earlier observation that the carbon content does not affect the Young modulus value. On the other hand, the results obtained by Speck [66] are lower than the results obtained by Brenton [56] and Jun [70], probably due to a higher porosity level in the specimen.

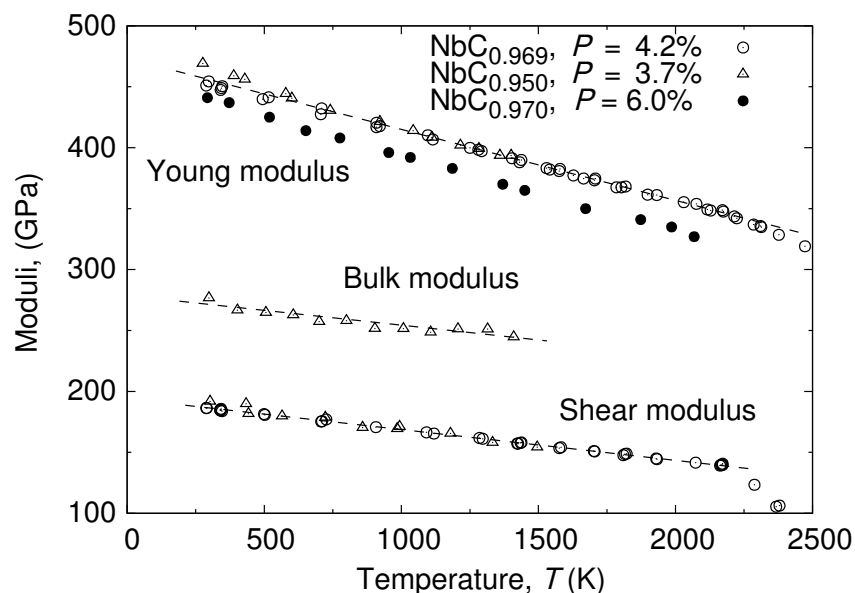


**Figure 12.** Young modulus as a function of the temperature: NbC<sub>0.969</sub>: [56]; NbC<sub>0.950</sub>: [70]; NbC<sub>0.970</sub>: [66]. P: porosity.

According to Brenton [56], the relationship between temperature and the Young modulus can be described by the equation:

$$E = E_{0T} - bT \exp\left(-\frac{T_0}{T}\right) \quad (7)$$

where  $b$ ,  $T_0$  and  $E_{0T}$  are constants. Using the data presented in Figure 12 for the NbC<sub>0.950</sub> and NbC<sub>0.969</sub> carbides and Equation (7), we can obtain the following values for the constants in the equation:  $E_{0T} = 473.443$ ,  $b = 0.0584528$  and  $T_0 = -0.358657$ .

The effect of the temperature on the shear modulus of the NbC carbide was studied by Brenton [56] and by Jun [70] (Figure 12). The shear modulus decreases linearly with temperature, and the results obtained by these two authors are very similar. According to Brenton [56], the relationship between the shear modulus and temperature can be described by the following equation:

$$G = B_1 - B_2T \quad (8)$$

where  $B_1$  and  $B_2$  are constants. The calculated values of the  $B_1$  and  $B_2$  constants are 194.439 and 0.0255038, respectively. The sudden drop observed in the shear modulus for temperature around 2100 K was attributed by the authors to grain boundary sliding [56]. The same sudden drop, although a less pronounced one, can be observed at the same temperature in Figure 12 for the values of the Young modulus.

Figure 13 shows how the Poisson coefficient varies with temperature as measured by Speck [66] and Jun [70]. The results obtained by Speck [66] are systematically lower than the ones obtained by Jun [70]. Another difference between the results shown in Figure 13 is that these results indicate

opposing trends of the variation of the Poisson coefficient with temperature. The full line in Figure 13 was calculated using Equations (7)–(9) below (which is valid for isotropic materials):

$$\nu = \frac{E}{2G} - 1 \quad (9)$$

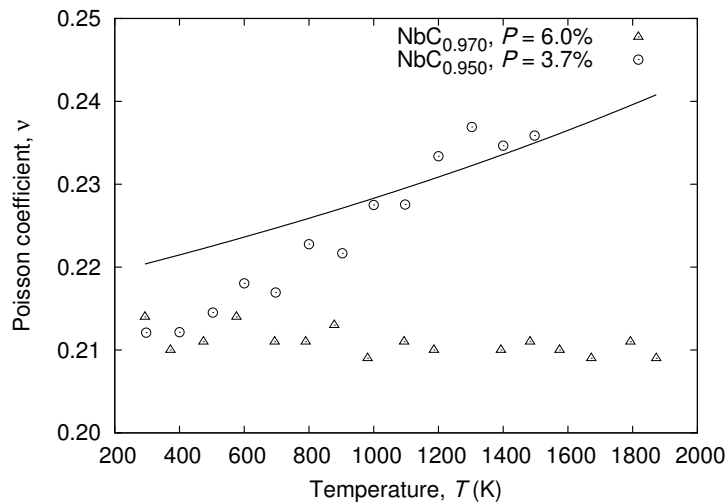


**Figure 13.** Poisson coefficient of the NbC carbide as a function of the temperature. NbC<sub>0.970</sub> ([66]); NbC<sub>0.950</sub> ([70]). P: porosity.

The calculated values show an increase in the Poisson coefficient with the temperature, but the agreement with the experimental values is very poor. The observations concerning the mechanical properties made above indicate that further investigation is necessary in order to fully understand the effects of porosity and stoichiometry.

Finally, the bulk modulus can be calculated from the values of  $E$  and  $G$  using the following equation:

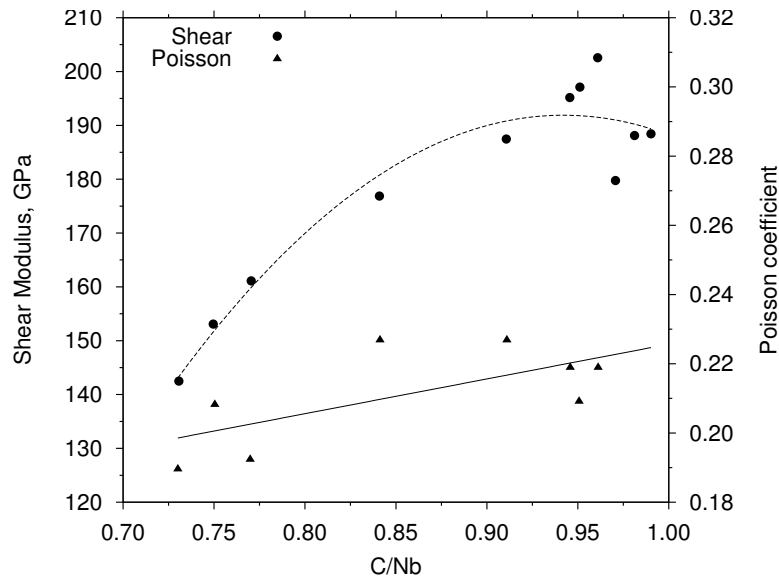
$$B = \frac{EG}{3(3G - E)} \quad (10)$$

Figure 12 indicates that the bulk modulus decreases with temperature, and the calculated values show an acceptable agreement with the experimental values.

More recent results of the elastic properties of the NbC were compiled by Kurlov [71] (Figure 14) as a function of the C/Nb ratio. The dependence of the shear modulus,  $G$ , and the Poisson coefficient,  $\nu$ , is given by ( $y$  is the C/Nb ratio):

$$G(y) = -709.1 + 1899.1y - 1000.8y^2 \text{ [GPa]} \quad (11)$$

$$\nu(y) = 0.1166 + 0.1169y \quad (12)$$



**Figure 14.** Variation of the shear modulus and Poisson's ratio of the NbC carbide as a function of the C/Nb ratio at 300 K ([71]).

## 5. Conclusions

The C-Nb binary system presents at least 02 different stable carbides: the cubic NbC carbide and the hexagonal Nb<sub>2</sub>C carbide. Both phases shows a great stoichiometric deviation due to the presence of carbon vacancies in the crystal structure. It is known that an ordered phase exists in this system, but the temperatures at which the order-disorder transition occurs have not been accurately determined.

The chemical bonding in the NbC carbide is very complex with a prevalent covalent characteristic, but also showing a metallic and ionic characteristic. The analysis of the bonding in this material allows an explanation for the remarkable combination of physical properties.

The lattice parameter of the NbC carbide varies non-linearly with its chemical composition, increasing as carbon content increases. The effect of vacancies on the lattice parameter is a complex phenomenon and involves the analysis of the displacement fields generated by vacancies.

The variation of the lattice parameter of NbC carbide with the temperature is rather insensitive to chemical composition changes. However, the literature shows conflicting results regarding the thermal expansion coefficient, and a systematic study of this property is needed in order to firmly establish this conclusion.

The mechanical properties of NbC carbide are determined from the measurements of the speed of sound in sintered specimens. The mechanical properties are strongly dependent on the specimen porosity, making it difficult to determine the intrinsic values of these properties and, also, their dependence with temperature and stoichiometry.

**Acknowledgments:** The authors would like to thank Mathias Woydt for his helpful suggestions.

**Author Contributions:** These authors contributed equally to this work.

**Conflicts of Interest:** The authors declare no conflict of interest.

## References

1. Williams, W.S. The thermal conductivity of metallic ceramics. *JOM* **1998**, *50*, 62–66.
2. Goldschmidt, H.J. *Interstitial Alloys*; Butterworth & Co: London, UK, 1967.
3. Gusev, A.I.; Rempel, A.A.; Magerl, A.J. *Disorder and Order in Strongly Nonstoichiometric Compounds: Transition Metal Carbides, Nitrides and Oxides*, 1st ed.; Springer: Heidelberg, Germany, 2010.

4. Llanos, L.; Pereda, B.; Lopez, B. Interaction between recovery, recrystallization, and NbC strain-Induced precipitation in high-Mn steels. *Metall. Mater. Trans. A* **2015**, *46*, 5248–5265.
5. Li, D.; Feng, Y.; Song, S.; Liu, Q.; Bai, Q.; Wu, G.; Lv, N.; Ren, F. Influences of Nb-microalloying on microstructure and mechanical properties of Fe-25Mn-3Si-3Al TWIP steel. *Mater. Des.* **2015**, *84*, 238–244.
6. Zhi, X.; Xing, J.; Fu, H.; Xiao, B. Effect of Niobium on the as-cast microstructure of hypereutectic high chromium cast iron. *Mater. Lett.* **2008**, *62*, 857–860.
7. Woydt, M.; Mohrbacher, H. The use of Niobium carbide (NbC) as cutting tools and for wear resistant tribosystems. *Int. J. Refract. Met. Hard Mater.* **2015**, *49*, 212–218.
8. Huang, S.G.; van der Biest, O.; Li, L.; Vleugels, J. Properties of NbC-Co cermets obtained by spark plasma sintering. *Mater. Lett.* **2007**, *61*, 574–577.
9. Nedfors, N.; Tengstrand, O.; Lewin, E.; Furlan, A.; Eklund, P.; Hultman, L.; Jansson, U. Structural, mechanical and electrical-contact properties of nanocrystalline-NbC/amorphous-C coatings deposited by magnetron sputtering. *Surf. Coat. Technol.* **2011**, *206*, 354–359.
10. Long, B.D.; Umamoto, M.; Todaka, Y.; Othman, R.; Zuhailawati, H. Fabrication of high strength Cu-NbC composite conductor by high pressure torsion. *Mater. Sci. Eng. A* **2011**, *528*, 1750–1756.
11. Shiri, S.G.; Abachi, P.; Pourazarang, K.; Rahvard, M.M. Preparation of in-situ Cu/NbC nanocomposite and its functionally graded behavior for electrical contact applications. *Trans. Nonferr. Met. Soc. China* **2015**, *25*, 863–872.
12. Zhong, Y.; Xia, X.; Shi, F.; Zhan, J.; Tu, J.; Fan, H.J. Transition metal carbides and nitrides in energy storage and conversion. *Adv. Sci.* **2016**, *3*, 1500286.
13. Michalsky, R.; Zhang, Y.J.; Peterson, A.A. Trends in the Hydrogen evolution activity of metal carbide catalysts. *ACS Catal.* **2014**, *4*, 1274–1278.
14. Meyer, S.; Nikiforov, A.V.; Petrushina, I.M.; Kohler, K.; Christensen, E.; Jensen, J.O.; Bjerrum, N.J. Transition metal carbides (WC, Mo<sub>2</sub>C, TaC, NbC) as potential electrocatalysts for the hydrogen evolution reaction (HER) at medium temperatures. *Int. J. Hydrog. Energy* **2015**, *40*, 2905–2911.
15. Storms, E.K.; Krikorian, N.H. The Niobium-Niobium carbide system. *J. Phys. Chem.* **1960**, *64*, 1471–1477.
16. Kimura, H.; Sasaki, Y. The phase diagram of the Niobium-Carbon system. *Trans. Jpn. Inst. Met.* **1961**, *2*, 98–104.
17. Smith, J.F.; Carlson, O.N.; de Avillez, R.R. The Niobium-Carbon system. *J. Nucl. Mater.* **1987**, *148*, 1–16.
18. Wiesenberger, H.; Lengauer, W.; Ettmayer, P. Reactive diffusion and phase equilibria in the Va-C, Nb-C, Ta-C and Ta-N systems. *Acta Mater.* **1998**, *46*, 651–666.
19. Kaufman, L.; Nesor, H. Coupled phase diagrams and thermochemical data for transition metal binary systems IV. *Calphad* **1978**, *2*, 295–318.
20. Balasubramanian, K.; Kirkaldy, J.S. Thermodynamics of nonstoichiometric B1 carbides and nitrides. *Calphad* **1985**, *9*, 103–115.
21. Ohtani, H.; Hasebe, M.; Nishizawa, T. Calculation of the Fe-C-Nb ternary phase diagram. *Calphad* **1989**, *13*, 183–204.
22. Okamoto, H. C-Nb (Carbon-Niobium). *J. Phase Equilib. Diff.* **1998**, *19*, 87.
23. Lee, B.J. Thermodynamic assessment of the Fe-Nb-Ti-C-N system. *Metall. Mater. Trans. A* **2001**, *32*, 2423–2439.
24. Kud', I.V.; Likhoded, L.S.; Eremenko, L.I.; Makarenko, G.N.; Fedorus, V.B.; Prilutskii, E.V. Features of (Ti, Me)C solid solution formation. *Powder Metall. Met. Ceram.* **2006**, *45*, 14–19.
25. Peng, Y.; Zhou, P.; Bu, M.; Zhang, W.; Du, Y. A thermodynamic evaluation of the C-Cr-Nb system. *Calphad* **2016**, *53*, 10–19.
26. Wijeyesekera, S.D.; Hoffmann, R. Transition metal carbides: A comparison of bonding in extended and molecular interstitial carbides. *Organometallics* **1984**, *3*, 949–961.
27. De Novion, C.H.; Maurice, V. III interstitial compounds: Order and disorder in carbides and nitrides. *J. Phys. Colloq.* **1977**, *38*, C7-211–C7-220.
28. De Novion, C.H.; Landesman, J.P. Order and disorder in transition metal carbides and nitrides: Experimental and theoretical aspects. *Pure Appl. Chem.* **1985**, *57*, 1391–1402.
29. Landesman, J.P.; Christensen, A.N.; Novion, C.H.D.; Lorenzelli, N.; Convert, P. Order-disorder transition and structure of the ordered vacancy compound Nb<sub>6</sub>C<sub>5</sub>: Powder neutron diffraction studies. *J. Phys. C* **1985**, *18*, 809–823.
30. Gusev, A.I.; Rempel, A.A. Vacancy distribution in ordered Me<sub>6</sub>C<sub>5</sub> type carbides. *J. Phys. C* **1987**, *20*, 5011–5025.

31. Rempel, A.A.; Gusev, A.I.; Belyaev, M.Y. 93 Nb NMR study of an ordered and a disordered non-stoichiometric Niobium carbide. *J. Phys. Colloq.* **1987**, *20*, 5655–5666.
32. Priem, T.; Beuneu, B.; de Novion, C.H.; Chevrier, J.; Livet, F.; Finel, A.; Lefevbre, S. Short-range order and static displacements in non-stoichiometric transition metal carbides and nitrides. *Phys. B* **1989**, *156–157*, 47–49.
33. Gusev, A.I. Order-disorder transformations and phase equilibria in strongly nonstoichiometric compounds. *Phys. Uspekhi* **2000**, *43*, 1–37.
34. Gusev, A.I.; Rempel, A.A. Phase diagrams of Metal-Carbon and Metal-Nitrogen systems and ordering in strongly nonstoichiometric carbides and nitrides. *Phys. Status Solidi A* **2001**, *163*, 273–304.
35. Gusev, A.I.; Rempel, A.A. Order-Disorder phase transition channel in Niobium carbide. *Phys. Status Solidi A* **2006**, *93*, 71–80.
36. Gusev, A. Sequence of phase transformations in the formation of superstructures of the  $M_6C_5$  type in nonstoichiometric carbides. *J. Exp. Theor. Phys.* **2009**, *109*, 417–433.
37. Kurlov, A.; Gusev, A. Ordering of nonstoichiometric hexagonal compounds  $M_2X$ : A sequence of special figures. *Phys. Solid State* **2009**, *51*, 2051–2057.
38. Gubanov, V.A.; Ivanovsky, A.L.; Zhukov, V.P. *Electronic Structure of Refractory Carbides and Nitrides*; Cambridge University Press: Cambridge, UK, 2005.
39. Benco, L. Metal-to-Metal bonding in transition metal monocarbides and mononitrides. *J. Solid State Chem.* **1997**, *128*, 121–129.
40. Hugosson, H.W.; Eriksson, O.; Jansson, U.; Johansson, B. Phase stabilities and homogeneity ranges in 4d-transition-metal carbides: A theoretical study. *Phys. Rev. B* **2001**, *63*, 134108.
41. Vojvodic, A.; Ruberto, C. Trends in bulk electron-structural features of rocksalt early transition-metal carbides. *J. Phys. Condens. Matter* **2010**, *22*, 375501.
42. Korir, K.K.; Amolo, G.O.; Makau, N.W.; Joubert, D.P. First-principle calculations of the bulk properties of 4d transition metal carbides and nitrides in the rocksalt, zinblende and wurtzite structures. *Diam. Relat. Mater.* **2011**, *20*, 157–164.
43. Momma, K.; Izumi, F. VESTA-3 for three-dimensional visualization of crystal, volumetric and morphology data. *J. Appl. Crystallogr.* **2011**, *44*, 1272–1276.
44. Toma, H. *Coordination Chemistry, Organometallics and Catalysis*; Blucher: São Paulo, Brazil, 2013. (In Portuguese)
45. Klein, B.M.; Papaconstantopoulos, D.A.; Boyer, L.L. Linear combination of atomic orbitals coherent potential approximation studies of Carbon vacancies in the substoichiometric refractory monocarbides  $NbC_x$ ,  $TaC_x$ , and  $HfC_x$ . *Phys. Rev. B* **1980**, *22*, 1946–1966.
46. Pickett, W.E.; Klein, B.M.; Zeller, R. Electronic structure of the Carbon vacancy in NbC. *Phys. Rev. B* **1986**, *34*, 2517–2521.
47. Krajewski, A.; D'Alessio, L.; de Maria, G. Physico-chemical and thermophysical properties of cubic binary carbides. *Cryst. Res. Technol.* **1998**, *33*, 341–374.
48. Jhi, S.; Louie, S.G.; Cohen, M.L.; Ihm, J. Vacancy hardening and softening in transition metal carbides and nitrides. *Phys. Rev. Lett.* **2001**, *86*, 3348–3351.
49. Rogovoi, Y. Effect of structural vacancies on the nature of metal-metal and metal-Carbon bonds in cubic monocarbides. *Powder Metall. Met. Ceram.* **1999**, *38*, 44–50.
50. Will, G.; Platzbecker, R. Crystal structure and electron density distribution in Niobium carbide. *Z. Anorg. Allg. Chem.* **2001**, *627*, 2207–2210.
51. Elliott, R.O.; Kempter, C.P. Thermal expansion of some transition metal carbides. *J. Phys. Chem.* **1958**, *62*, 630–631.
52. Storms, E.K.; Krikorian, N.H. The variation of lattice parameter with Carbon content of Niobium carbide. *J. Phys. Chem.* **1959**, *63*, 1747–1749.
53. Kempter, C.P.; Storms, E.K.; Fries, R.J. Lattice dimensions of NbC as a function of stoichiometry. *J. Chem. Phys.* **1960**, *33*, 1873–1874.
54. Brown, H.L.; Armstrong, P.E.; Kempter, C.P. Elastic properties of some polycrystalline transition-metal monocarbides. *J. Chem. Phys.* **1966**, *45*, 547–549.
55. Kempter, C.P.; Storms, E.K. Thermal expansion of some Niobium carbides. *J. Less Common Met.* **1967**, *13*, 443–447.

56. Brenton, R.F.; Saunders, C.R.; Kempter, C.P. Elastic properties and thermal expansion of Niobium mono-carbide to high temperatures. *J. Less Common Met.* **1969**, *19*, 273–278.
57. Jun, C.K.; Shaffer, P.T.B. Thermal expansion of Niobium carbide, Hafnium carbide and Tantalum carbide at high temperatures. *J. Less Common Met.* **1971**, *24*, 323–327.
58. Kaufmann, R.; Meyer, O. Ion channeling in NbC<sub>1-c</sub>: Determination of local atomic displacements around Carbon vacancies. *Phys. Rev. B* **1983**, *28*, 6216–6226.
59. Metzger, T.H.; Peisl, J.; Kaufmann, R. X-ray determination of local atomic displacements around Carbon vacancies in NbC<sub>1-c</sub> single crystals. *J. Phys. F* **1983**, *13*, 1103–1113.
60. Zaoui, A.; Kacimi, S.; Zaoui, M.; Bouhafs, B. Vacancy effects on structural and electronic properties of 4d transition-metal carbides. *Comput. Mater. Sci.* **2009**, *44*, 1071–1075.
61. Ordan'yan, S.S.; Avgustinik, A.I.; Kudryasheva, L.V. Densification of nonstoichiometric Niobium-carbide phases. *Powder Metall. Met. Ceram.* **1968**, *7*, 612–618.
62. Ajami, F.; MacCrone, R. Thermal expansion, Debye temperature and Gruneisen constant of carbides and nitrides. *J. Less Common Met.* **1974**, *38*, 101–110.
63. Samsonov, G.V. Imperfection of Carbon sublattice: Effect on the properties of refractory carbides of transition metals. *Powder Metall. Met. Ceram.* **2008**, *47*, 13–20.
64. Houska, C.R. Thermal expansion of certain group IV and group V carbides at high temperatures. *J. Am. Ceram. Soc.* **1964**, *47*, 310–311.
65. Levinson, L.S. High-temperature heat content of Niobium carbide and of Tantalum carbide. *J. Chem. Phys.* **1963**, *39*, 1550–1551; Corrected in *J. Chem. Phys.* **1965**, *42*, 3342.
66. Kral, C.; Lengauer, W.; Rafaja, D.; Etmayer, P. Critical review on the elastic properties of transition metal carbides, nitrides and carbonitrides. *J. Alloy. Compd.* **1998**, *265*, 215–233.
67. Ledbetter, H.M.; Chevacharoenkul, S.; Davis, R.F. Monocrystal elastic constants of NbC. *J. Appl. Phys.* **1986**, *60*, 1614–1617.
68. Olevsky, E.A.; Kandukuri, S.; Froyen, L. Consolidation enhancement in spark-plasma sintering: Impact of high heating rates. *J. Appl. Phys.* **2007**, *102*, 114913.
69. Woydt, M.; Mohrbacher, H. Friction and wear of binder-less niobium carbide. *Wear* **2013**, *306*, 126–130.
70. Jun, C.K.; Shaffer, P.T.B. Elastic moduli of Niobium carbide and Tantalum carbide at high temperature. *J. Less Common Met.* **1971**, *23*, 367–373.
71. Kurlov, A.S.; Gusev, A.I. Accounting for non-stoichiometry of niobium carbide NbCy upon milling to a nanocrystalline state. *Phys. Solid State* **2013**, *55*, 2522–2530.



© 2016 by the authors; licensee MDPI, Basel, Switzerland. This article is an open access article distributed under the terms and conditions of the Creative Commons Attribution (CC-BY) license (<http://creativecommons.org/licenses/by/4.0/>).